Bioorganic & Medicinal Chemistry xxx (xxxx) xxx–xxx

Contents lists available at ScienceDirect

Bioorganic & Medicinal Chemistry

journal homepage: www.elsevier.com/locate/bmc

Nitric oxide donor-based FFA1 agonists: Design, synthesis and biological evaluation as potential anti-diabetic and anti-thrombotic agents

Zheng Li[a,*], Xue Xu[b], Roujia Liu[a], Fengjian Deng[a], Xiaohua Zeng[a], Luyong Zhang[a,c,d,*]

[a] School of Pharmacy, Guangdong Pharmaceutical University, Guangzhou 510006, PR China
[b] Guangzhou General Pharmaceutical Research Institute Co., Ltd, Guangzhou 510240, PR China
[c] Guangzhou Key Laboratory of Construction and Application of New Drug Screening Model Systems, Guangdong Pharmaceutical University, Guangzhou 510006, PR China
[d] Jiangsu Key Laboratory of Drug Screening, China Pharmaceutical University, Nanjing 210009, PR China

ARTICLE INFO

Keywords:
Cardiovascular complications
Diabetes
FFA1
Hybrid
NO donor

ABSTRACT

The cardiovascular complications were highly prevalent in type 2 diabetes mellitus (T2DM), even at the early stage of T2DM or the state of intensive glycemic control. Thus, there is an urgent need for the intervention of cardiovascular complications in T2DM. Herein, the new hybrids of FFA1 agonist and NO donor were design to obtain dual effects of anti-hyperglycemic and anti-thrombosis. As expected, the induced-fit docking study suggested that it is feasible for our design strategy to hybrid NO donor with compound **1**. These hybrids exhibited moderate FFA1 agonistic activities and anti-platelet aggregation activities, and their anti-platelet effects mediated by NO were also confirmed in the presence of NO scavenger. Moreover, compound **3** revealed significantly hypoglycemic effect and even stronger than that of TAK-875 during an oral glucose tolerance test in mice. Potent and multifunctional hybrid, such as compound **3**, is expected as a potential candidate with additional cardiovascular benefits for the treatment of T2DM.

1. Introduction

Type 2 diabetes mellitus (T2DM) is a life-long disease characterized by insulin deficiency and peripheral insulin resistance.[1,2] There is an inspiring array of anti-diabetic drugs for maintaining the stabilization of plasma glucose.[3–6] However, current researches suggested that cardiovascular complications were highly prevalent in diagnosed and undiagnosed T2DM, even at the early stage of T2DM or the state of intensive glycemic control.[7,8] Therefore, a new hypoglycemic drug with additional cardiovascular benefits is an unmet clinical need for T2DM.

The long-chain free fatty acid receptor 1 (FFA1, previously known as GPR40), a new anti-diabetic target mainly located in pancreatic β-cells, enhances the glucose-stimulated insulin secretion without the risk of hypoglycemia.[9–12] Thus, there is an advantage for FFA1 agonists for the treatment of T2DM. Currently, many FFA1 agonists derived from phenylpropionic acid moiety have been reported (Fig. 1),[13–21] and several clinical trials were performed to assess the efficacy and safety of TAK-875 and AMG-837 as anti-diabetic drugs.[22,23] To enlarge the structural diversity of FFA1 agonists, different scaffolds were explored in our previous studies.[24–32]

Nitric oxide (NO), a well-known signaling molecule, plays an important role in a variety of physiological processes in cardiovascular system, such as the relaxation of vascular smooth muscle, inhibition of platelet aggregation, reduced adherence and activation of neutrophil.[33–35] Accordingly, we hypothesize that the hybirds of NO donor and FFA1 agonists may provide new agents with dual effects on anti-hyperglycemic and anti-thrombosis, and thereby obtaining additional cardiovascular benefits.

Herein, our previously reported phenoxyacetic acid derivative **1** was selected due to its better glucose-lowering effect than TAK-875, and the modifiable 4-position (green mark in Fig. 2) identified by the molecular modeling and structure-activity relationship studies.[13,14] The new hybrids of NO donor and compound **1** were synthesized to verify our hypothesis above (Fig. 2). Indeed, these hybrids revealed the dual effects on anti-hyperglycemic and anti-thrombosis.

2. Results and discussion

2.1. Chemistry

The synthesis of compounds **2–4** is depicted in Scheme 1. The intermediate **5a** was synthesized *via* our previously reported procedure.[13]

* Corresponding authors at: School of Pharmacy, Guangdong Pharmaceutical University, Guangzhou 510006, PR China (L. Zhang).
E-mail addresses: lizhengdrug@gdpu.edu.cn (Z. Li), lyzhang@cpu.edu.cn (L. Zhang).

https://doi.org/10.1016/j.bmc.2018.07.050
Received 18 June 2018; Received in revised form 27 July 2018; Accepted 30 July 2018

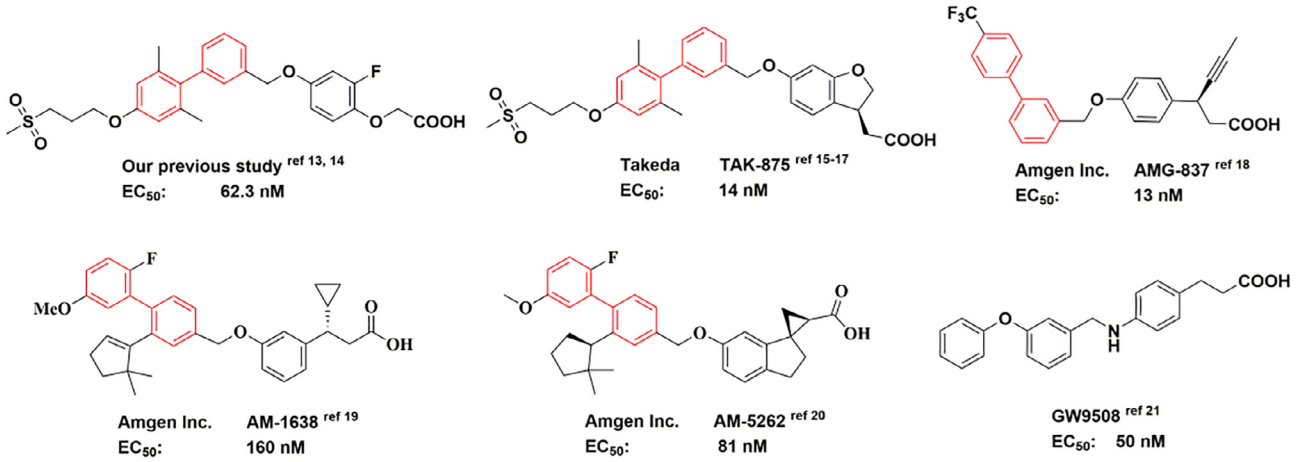

Fig. 1. Synthetic FFA1 agonists derived from phenylpropionic acid moiety.

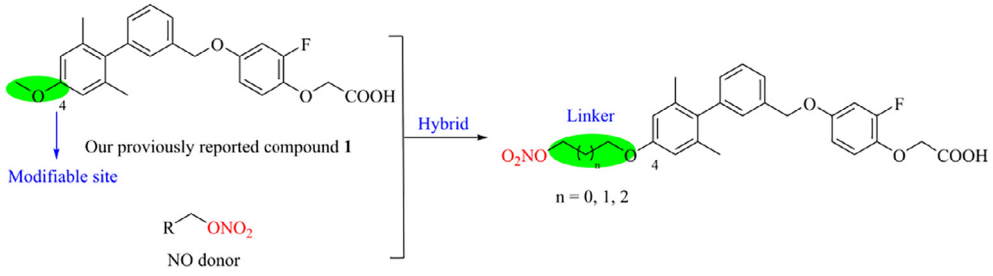

Fig. 2. The hybrid strategy of NO donor and FFA1 agonist **1**.

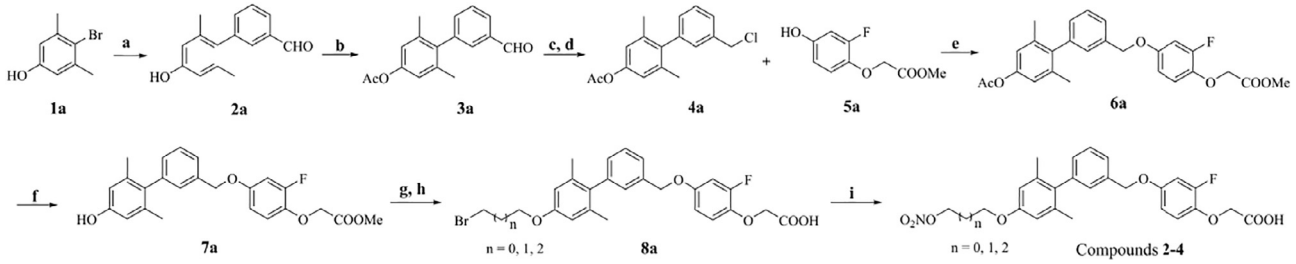

Scheme 1. Synthesis of target compounds **2–4**. Reagents and conditions: (a) (3-formylphenyl)boronic acid, $Pd(PPh_3)_4$, Na_2CO_3, toluene, ethanol, H_2O, 80 °C, 12 h, 85%; (b) AcCl, NEt_3, CH_2Cl_2, 0 °C, 2 h, 95%; (c) $NaBH_4$, CH_3OH, THF, 0 °C, 30 min; (d) $SOCl_2$, CH_2Cl_2, DMF, 40 °C, 4 h, 79% (two steps); (e) K_2CO_3, acetone, KI, reflux, 12 h, 77%; (f) CH_3ONa, MeOH, r.t., 2 h, 87%; (g) RBr, K_2CO_3, acetone, reflux, 12 h; (h) $LiOH{\cdot}H_2O$, THF/MeOH/H_2O, r.t., 4 h; (i) $AgNO_3$, CH_3CN, reflux, 2 h, 27%–39%.

Table 1
FFA1 agonistic activities and selected parameters of hybrids.

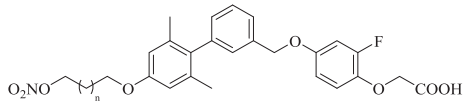

Compd.	n	EC_{50} (nM)[a]	cLogP[b]	tPSA[c]
TAK-875		32.5	4.697	99.13
1		54.2	5.426	64.99
2	0	76.4	3.206	126.03
3	1	61.5	3.49	126.03
4	2	93.7	3.205	126.03

[a] EC_{50} values represent the mean of three independent determinations.
[b] clogP values were estimated with ChemDraw Ultra, version 12.0.
[c] Topological polar surface area was calculated using ChemDraw Ultra, version 12.0.

The key intermediate **3a** was derived from the acetylation of intermediate **2a**, which was prepared by classical Suzuki coupling of (3-formylphenyl)boronic acid with 4-bromo-3,5-dimethylphenol in the presence of $Pd(PPh_3)_4$. The aldehyde in intermediate **3a** was reduced by $NaBH_4$, followed by treating with $SOCl_2$ to provide intermediate **4a**. Condensation of **4a** with **5a** by Williamson ether synthesis afforded intermediate **6a**, and the deacetylation of **6a** in the presence of sodium methoxide gives phenol **7a**. After stirring at reflux, the phenol **7a** was alkylated in acetone, followed by basic hydrolysis, given intermediate **8a**. The S_N2 reaction of silver nitrate with intermediate **8a** in acetonitrile afforded the target compounds **2–4**.

2.2. FFA1 agonistic activity and molecular modeling study

Aiming to obtain the additional cardiovascular benefits, we hypothesize that the hybrids of NO donor and phenoxyacetic acid derivative **1** might have dual effects on anti-hyperglycemic and anti-thrombosis. The *in vitro* FFA1 agonistic activities of synthesized hybrids were evaluated by a fluorometric imaging plate reader (FLIPR) assay.

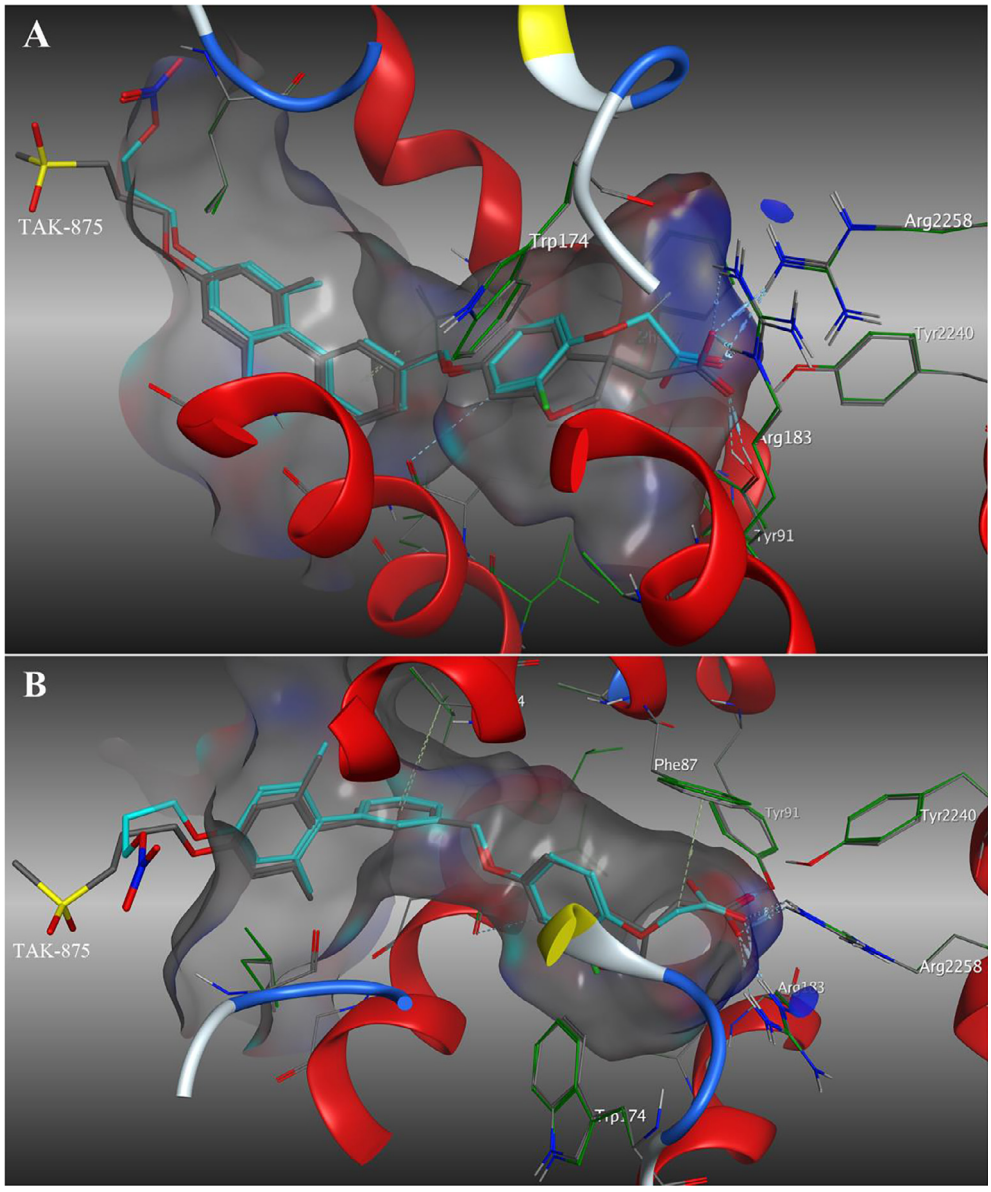

Fig. 3. The frontal view (A) and side-view (B) in docking model of compound **3** (cyan carbon) in crystal structure of hFFA1. Key residues are labeled in white, TAK-875 is represented by gray, and hydrogen bonding interactions are represented by silvery dashed lines.

Besides, cLogP and tPSA values were also monitored during the process of structural optimization. As shown in Table 1, the direct hybrid **2** of NO donor nitrate and compound **1** revealed a slightly reduced agonistic activity compared with compound **1**, despite a lower cLogP value and larger tPSA value attributed to the hydrophily of nitrate. Gratifyingly, a significantly increased activity was obtained only by incorporating a methylene (compound **3**). However, further extending the length of linker with methylene appeared to diminish the agonistic activity to some extent (compound **4** *vs* **2** or **3**).

To understand the interaction mode of hybrids, an induced-fit docking study of compound **3** was performed using the crystal structure (PDB code: 4PHU) of FFA1.[36] As shown in Fig. 3, compound **3** fit well into the binding site of TAK-875 with slightly rotated phenoxyacetic acid, which formed a δ-π interaction with benzene of Phe87 despite losing a hydrogen bond with hydroxyl of Tyr91. The missing of interaction from Tyr91 might explain that the difference of potency between compound **3** and TAK-875. As expected, the NO donor at the terminal phenyl group was exposed to the outside of binding pocket, which could tolerate a variety of linkers. This result suggested that it is feasible for our design strategy to hybrid NO donor with compound **1** at the modifiable 4-position of terminal phenyl group.

2.3. Anti-platelet aggregation activity and NO release

The anti-platelet aggregation activities of hybrids (0.1 mM) were performed on the ADP-induced platelet aggregation in rabbit platelet rich plasma by using Born's turbidimetric method.[37] Ticlopidine was selected as positive control. As shown in Fig. 4, compounds **2**, **3** and **4** inhibited the ADP-induced platelet aggregation by 8.28%, 10.76% and 11.12%, respectively, which were much stronger than that of parent compound **1**. This result suggested that the incorporation of NO donor improved the inhibitory effect on the ADP-induced platelet aggregation. To confirm our speculation above, the carboxy-PTIO (a NO scavenger) was then incubated with the drug-platelet suspension and tested for inhibitory activity. Indeed, the anti-platelet effects of compounds **2**, **3** and **4** were decreased from 8.28%, 10.76% and 11.12% to 1.34%, 1.05% and 1.15% by treatment with carboxy-PTIO (20 μM), respectively. These results further clarified our design strategy to introduce

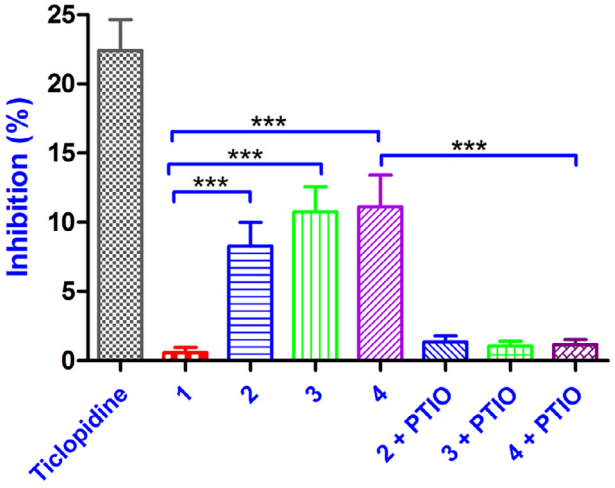

Fig. 4. *In vitro* inhibitory effects for ADP-induced rabbit platelet aggregation. Rabbit platelet suspensions were pre-incubated with tested compounds (0.1 mM) at 37 °C for 5 min followed by addition of ADP (10 μM). Carboxy-PTIO (20 μM) was added and incubated with the drug-platelet suspension in the indicated group. Results are expressed as means (%) ± SD of each group from three independent experiments. $^{***}p \leq 0.001$ were analyzed using a one-way ANOVA with Tukey's multiple-comparison post hoc test.

the NO donor for improving the anti-platelet effect, and support our hypothesis on the hybrids with dual effects on anti-hyperglycemic and anti-thrombosis.

In order to further confirm whether compound **3** could induce the release of NO in the concentration- and time-dependent manner, we determined the levels of NO induced by compound **3** at the concentration of 0.03, 0.1, 0.2, and 0.3 mM by using Griess assay.[38] As shown in Fig. 5, the compound **3** induce the release of NO at the concentration- and time-dependent manner. With the concentration of compound **3** increased, the total levels of NO and the time to peak were increased.

2.4. Oral glucose tolerance test of compound *3*

Based on the better balance between anti-platelet aggregation and FFA1 agonistic activity, compound **3** was selected to evaluate its glucose-lowering effects *in vivo* (Fig. 6). Interestingly, compound **3** (20 mg/kg) significantly suppressed the plasma glucose excursion by 41.6%, and the hypoglycemic effect was stronger than that of TAK-875 (−32.3%) despite an inferior agonistic activity for compound **3** *in vitro*. These results indicated that compound **3** has the dual effects on the inhibition of platelet aggregation and the robust glucose-lowering effect, which might provide some additional cardiovascular benefits during the intensive glycemic control.

3. Conclusion

Aiming to obtain the additional cardiovascular benefits, the design strategy of incorporating NO donor with FFA1 agonist was developed to achieve dual effects of anti-hyperglycemic and anti-thrombosis. Indeed, three hybrids of FFA1 agonist **1** and nitrate revealed considerable FFA1 agonistic activities and anti-platelet aggregation activities. Moreover, the anti-platelet effects of NO donor in hybrids were eliminated by introducing NO scavenger carboxy-PTIO. The induced-fit docking study also suggested that it is successful to design hybrids at the modifiable site of compound **1**. During oral glucose tolerance test, compound **3** revealed significantly glucose-lowering effects and even stronger than that of TAK-875, the most representative FFA1 agonist. Altogether, compound **3** appears as a promising candidate with dual effects, and further studies based on the hybrid strategy will provide us more competitive hypoglycemic agent with additional cardiovascular benefits.

4. Experimental section

4.1. Chemistry

All commercial available materials and reagents were used without purification unless otherwise indicated. Purification by column chromatography was carried out using silica gel (200–300 mesh). Melting points were determined on a RY-1 melting-point apparatus and were uncorrected. The NMR spectra (300 MHz for ^{1}H NMR, 75 MHz for ^{13}C NMR spectra) were detected on Bruker ACF-300Q instrument. Chemical shifts are showed as values relative to internal standard (tetramethylsilane), and coupling constants (*J* values) were given in hertz (Hz). LC/MS spectra were determined on Waters liquid chromatography-mass spectrometer system (ESI). Elemental analyses were carried out by Heraeus CHN-O-Rapid analyzer. TAK-875 was synthesized via published procedures.[15]

4.1.1. 4′-Hydroxy-2′,6′-dimethyl-3-biphenylcarbaldehyde (*2a*)

The 4-bromo-3,5-dimethylphenol (5 g, 25.0 mmol) and (3-formylphenyl)boronic acid (3.8 g, 25.0 mmol) were dissolved in a mixture of 1 M sodium carbonate aq. (15 mL), EtOH (5 mL) and toluene (15 mL). After nitrogen substitution, $Pd(PPh_3)_4$ (0.05 equiv) was added. The reaction mixture was stirred at 80 °C under nitrogen atmosphere for 12 h. The reaction mixture was cooled, and water (15 mL) was added. The mixture was diluted with AcOEt (15 mL), and the insoluble material was filtered off through Celite. The organic layer of the filtrate was washed with brine, dried over anhydrous Na_2SO_4, and concentrated in

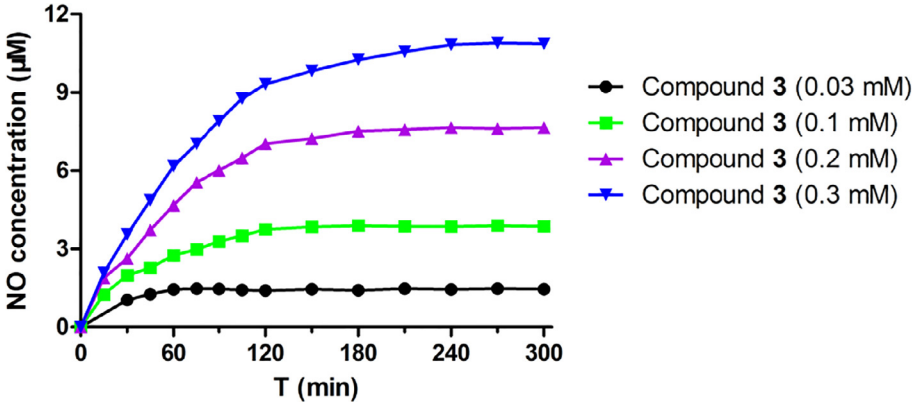

Fig. 5. NO-releasing assay of compound **3** at the concentration of 0.03, 0.1, 0.2, and 0.3 mM. The levels of NO presented as nitrite were measured by Griess assay and calculated according to the standard curve of nitrite. Data are expressed as the means of NO concentration at each time point.

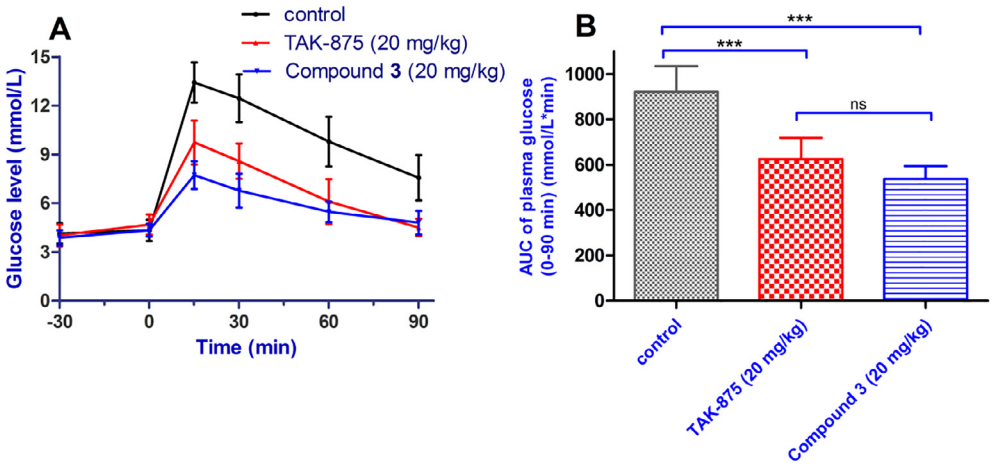

Fig. 6. Effects of compound **3** during OGTT in fasting ICR mice. (A) represented time-dependent changes of blood glucose levels after oral administration of test compounds, followed by oral glucose load (3 g/kg), respectively. (B) represented $AUC_{0-90min}$ of plasma glucose levels. Results are mean ± SD (n = 6 per group). $^{***}p \leq 0.001$ were analyzed using a one-way ANOVA with Tukey's multiple-comparison post hoc test.

vacuo. The residue was purified by silica gel column chromatography using a mixture of petroleum ether/ethyl acetate (10:1, v/v) as eluent to afford the desired product as a white solid (4.8 g, 85%). ^{1}H NMR (300 MHz, $CDCl_3$) δ: 10.05 (s, 1H), 7.86 (dd, J = 1.5, 7.7 Hz, 1H), 7.66 (t, J = 1.5 Hz, 1H), 7.59 (t, J = 7.7 Hz, 1H), 7.42 (dd, J = 1.5, 7.7 Hz, 1H), 6.62 (s, 2H), 4.69 (s, 1H), 1.97 (s, 6H).

*4.1.2. 3′-Formyl-2,6-dimethyl-[1,1′-biphenyl]-4-yl acetate (**3a**)*

To a solution of **2a** (4 g, 17.7 mmol) in CH_2Cl_2 (20 mL) was added Et_3N (2.7 g, 26.6 mmol), and this mixture was cooled to −3 °C. Subsequently, the acetyl chloride (2.1 g, 26.6 mmol) in CH_2Cl_2 (10 mL) was added in dropwise at a rate to ensure that the temperature did not exceed 0 °C. The reaction mixture was stirred for another 2 hrs at ambient temperature, then washed successively with 10% HCl (25 mL), 10% $NaHCO_3$ (25 mL) and brine (2 × 20 mL). The organic layer was dried over anhydrous Na_2SO_4, filtered and the solvent was then evaporated to give the desired products as colorless oil (4.5 g, 95%). ^{1}H NMR (300 MHz, $CDCl_3$) δ: 10.05 (s, 1H), 7.89 (d, J = 7.7 Hz, 1H), 7.67 (s, 1H), 7.61 (t, J = 7.6 Hz, 1H), 7.43 (d, J = 7.6 Hz, 1H), 6.86 (s, 2H)), 2.32 (s, 3H), 2.00 (s, 6H).

*4.1.3. 3′-(Chloromethyl)-2,6-dimethyl-[1,1′-biphenyl]-4-yl acetate (**4a**)*

To a solution of **3a** (4.0 g, 14.9 mmol) in MeOH (10 mL) and THF (20 mL) was added portionwise sodium borohydride (1.7 g, 44.7 mmol) at 0 °C and the mixture was stirred at 0 °C for 6 h. The reaction mixture was pouring into ice water (10 mL), and extracted with ethyl acetate (3 × 15 mL), the organic fractions were combined, washed with saturated brine (2 × 15 mL) prior to drying over anhydrous Na_2SO_4. After filtration and concentrate using a rotary evaporator, the residue was used in the next step without further purification. To a solution of the obtained solid in dichloromethane (20 mL) was slowly added thionyl chloride (5.3 g, 44.7 mmol) and a catalytic amount of DMF at room temperature. After stirring at 40 °C for 4 h, the reaction was concentrated under reduced pressure. The residue was purified by silica gel column chromatography using a mixture of petroleum ether/ethyl acetate (20:1, v/v) as eluent to afford the title compound (3.4 g, 79%). ^{1}H NMR (300 MHz, $CDCl_3$) δ: 7.44–7.39 (m, 1H), 7.34 (d, J = 7.9 Hz, 1H), 7.14(s, 1H), 7.10–7.06 (m, 1H), 6.82 (s, 2H), 4.52 (s, 2H), 2.31 (s, 3H), 1.97 (s, 6H).

*4.1.4. Methyl 2-(4-((4′-acetoxy-2′,6′-dimethyl biphenyl-3-yl)methoxy)-2-fluorophenoxy)acetate (**6a**)*

To a solution of **4a** (3.0 g, 10.4 mmol) and **5a** (2.1 g, 10.4 mmol) in acetone was added K_2CO_3 (2.9 g, 20.8 mmol) and a catalytic amount of KI at room temperature. The reaction mixture was heated to reflux with stirring overnight. Then the reaction mixture was cooled to room temprature followed by filtration and the filtrate was concentrated under vacuum. The residue was purified by silica gel column chromatography using a mixture of petroleum ether/ethyl acetate (7:1, v/v) as eluent to afford a white solid (3.6 g, 77%). ^{1}H NMR (300 MHz, DMSO-d_6) δ: 7.36–7.26 (m, 2H), 6.97–6.91 (m, 3H), 6.66 (d, J = 9.0 Hz, 1H), 6.42–6.38 (m, 3H), 5.01 (s, 2H), 4.69 (s, 2H), 3.59 (s, 3H), 2.32 (s, 3H), 1.79 (s, 6H).

*4.1.5. Methyl 2-(2-fluoro-4-((4′-hydroxy-2′,6′-dimethyl biphenyl-3-yl) methoxy)phenoxy)acetate (**7a**)*

To a solution of **6a** (3.5 g, 7.7 mmol) in CH_3OH was added CH_3ONa (0.5 g, 9.3 mmol) in small portions. The reaction mixture was stirred for 2 h at room temperature and then quenched with 1 N HCl (20 mL). The mixture was extracted with ethyl acetate (3 × 15 mL), and the combined organic phases were washed with brine (2 × 15 mL), dried and filtered. The filtrate was evaporated under vacuum and the residue was purified by column chromatography using a mixture of petroleum ether/ethyl acetate (5:1, v/v) as eluent to afford a white solid (2.8 g, 87%). ^{1}H NMR (300 MHz, DMSO-d_6) δ: 7.36–7.26 (m, 2H), 7.05 (s, 1H), 6.97–6.91 (m, 3H), 6.66 (d, J = 9.0 Hz, 1H), 6.42–6.38 (m, 3H), 5.01 (s, 2H), 4.69 (s, 2H), 3.59 (s, 3H), 1.79 (s, 6H).

*4.1.6. General procedure for synthesis of compounds **2–4***

To a solution of **7a** (1.0 equiv) in acetone was added the corresponding bromoalkane (1.0 equiv) and K_2CO_3 (2.0 equiv). The reaction mixture was reflux for 12 h, and then cooled to room temperature and filtered. The filtrate was concentrated under reduced pressure and the resultant residue was redissolved in ethyl acetate and washed with brine. The organic layer was dried over Na_2SO_4, filtered, and concentrated under reduced pressure. The residue was purified by column chromatography using a mixture of petroleum ether/ethyl acetate (5:1, v/v) as eluent to afford a white solid. The solid in THF/MeOH/H_2O (2: 3: 1) was added $LiOH{\cdot}H_2O$ (1.2 equiv), and the resulting mixture was stirred at room temperature for 4 h. The volatiles were removed under reduced pressure, and the residue was acidified with 1 N hydrochloric acid solution, and then filtered and the filter cake was washed with 5 mL of water, dried in vacuum to afford a white powder **8a**. To a solution of **8a** (1.0 equiv) in acetonitrile was added silver nitrate (1.5 equiv). The reaction mixture was stirred at reflux for 2 h under dark condition, and then cooled to room temperature and filtered. The filtrate was concentrated under reduced pressure and the resultant residue was purified by column chromatography using a mixture of petroleum ether/ethyl acetate (2:1, v/v) as eluent to afford the target compounds **2–4**.

*4.1.7. 2-(4-((2′,6′-Dimethyl-4′-(2-(nitrooxy)ethoxy)-[1,1′-biphenyl]-3-yl) methoxy)-2-fluorophenoxy)acetic acid (**2**)*

Yield: 35%; m.p. 112–114 °C; ^{1}H NMR (300 MHz, DMSO-d_6) δ:

7.49–7.42 (m, 2H), 7.18 (s, 1H), 7.07 (d, J = 8.8 Hz, 1H), 7.02–6.96 (m, 2H), 6.77 (t, d, J = 9.0 Hz, 1H), 6.69 (s, 2H), 5.09 (s, 2H), 4.74 (s, 2H), 4.66 (t, J = 6.0 Hz, 2H), 4.43 (t, J = 6.0 Hz, 2H), 1.91(s, 6H); ^{13}C NMR (75 MHz, DMSO-d_6) δ: 170.3, 157.5, 153.7, 152.3, 140.5, 139.7, 136.4, 133.5, 128.6, 128.8, 128.3, 125.9, 115.8, 112.7, 110.5, 104.2, 73.6, 69.7, 66.8, 65.7, 20.6; ESI-MS m/z: 484.1 $[M-H]^-$; Anal. calcd. For $C_{25}H_{24}FNO_8$: C, 61.85; H, 4.98; N, 2.89; Found: C, 61.81; H, 4.97; N, 2.88.

4.1.8. 2-(4-((2′,6′-Dimethyl-4′-(3-(nitrooxy)propoxy)-[1,1′-biphenyl]-3-yl)methoxy)-2-fluorophenoxy)acetic acid (3)

Yield: 27%; m.p. 105–107 °C; ^{1}H NMR (300 MHz, DMSO-d_6) δ: 7.48–7.42 (m, 2H), 7.19 (s, 1H), 7.06 (d, J = 8.8 Hz, 1H), 7.02–6.97 (m, 2H), 6.78 (t, d, J = 9.0 Hz, 1H), 6.69 (s, 2H), 5.09 (s, 2H), 4.74 (s, 2H), 4.58 (t, J = 6.1 Hz, 2H), 4.33 (t, J = 6.1 Hz, 2H), 2.17–2.13 (m, 2H), 1.91(s, 6H); ^{13}C NMR (75 MHz, DMSO-d_6) δ: 170.1, 157.9, 153.5, 152.5, 140.2, 139.7, 136.4, 133.5, 128.6, 128.8, 128.3, 125.9, 115.8, 112.7, 110.5, 104.2, 71.5, 69.7, 65.7, 64.3, 26.7, 20.8; ESI-MS m/z: 498.1 $[M-H]^-$; Anal. calcd. For $C_{26}H_{26}FNO_8$: C, 62.52; H, 5.25; N, 2.80; Found: C, 62.56; H, 5.24; N, 2.81.

4.1.9. 2-(4-((2′,6′-Dimethyl-4′-(4-(nitrooxy)butoxy)-[1,1′-biphenyl]-3-yl)methoxy)-2-fluorophenoxy)acetic acid (4)

Yield: 39%; m.p. 109–111 °C; ^{1}H NMR (300 MHz, DMSO-d_6) δ: 7.47–7.42 (m, 2H), 7.16 (s, 1H), 7.08 (d, J = 8.8 Hz, 1H), 7.01–6.95 (m, 2H), 6.76 (t, d, J = 9.1 Hz, 1H), 6.69 (s, 2H), 5.09 (s, 2H), 4.74 (s, 2H), 4.38 (t, J = 6.0 Hz, 2H), 4.12 (t, J = 6.0 Hz, 2H), 1.93 (s, 6H), 1.87–1.82 (m, 2H), 1.65–1.62 (m, 2H); ^{13}C NMR (75 MHz, DMSO-d_6) δ: 170.3, 157.9, 153.3, 152.5, 140.2, 139.7, 136.7, 133.5, 128.6, 128.5, 128.1, 125.9, 115.8, 112.7, 110.5, 104.5, 74.6, 69.7, 68.3, 65.7, 27.5, 23.4, 20.6; ESI-MS m/z: 512.1 $[M-H]^-$; Anal. calcd. For $C_{27}H_{28}FNO_8$: C, 63.15; H, 5.50; N, 2.73; Found: C, 63.18; H, 5.51; N, 2.72.

4.2. Molecular modeling

MOE (version 2014.0901, The Chemical Computing Group, Montreal, Canada) was used to perform the docking modeling based on the reported crystal structure of hFFA1 (PDB ID: 4PHU). Prior to molecular docking, other crystallized ligands and water were removed, and the obtained protein was performed by Protonate 3D prior to the Gaussian Contact surface was draw around the binding pocket of TAK-875. Subsequently, the binding pocket with Gaussian Contact surface was isolated. Compound **3** was induced-fit docked into the binding pocket and ranked with London dG scoring function. For energy minimization in binding pocket, MOE Forcefield Refinement was performed and ranked with London dG scoring function.

4.3. Ca^{2+} influx activity of CHO cells stably expressing human FFA1 (FLIPR Assay)

CHO cells stably expressing human FFA1 were plated at a density of 15 K cells/well and incubated 12 h in 5% CO_2 at 37 °C. Subsequently, culture medium was removed and washed with Hank's Balanced Salt Solution (100 μL). Then, cells were incubated in loading buffer (recording medium containing 2.5 μg/mL fluorescent calcium indicator Fluo 4-AM, 0.1% fatty acid-free BSA and 2.5 mmol/L probenecid) for 1 h at 37 °C. Various concentrations of test compounds or γ-linolenic acid (Sigma) were added into the cells, and the intracellular Ca^{2+} flux signals after addition were monitored by FLIPR Tetra system (Molecular Devices) for 90 s. The agonistic activities of test compounds on human FFA1 were expressed as [(A − B)/(C − B)] × 100 (increase of the intracellular calcium concentration (A) in the test compounds-treated cells and (B) in vehicle-treated cells, and (C) in 10 μM γ-linolenic acid-treated cells).

4.4. Animals and statistical analysis of the data

Rabbits and mice were purchased from Guangdong Medical Laboratory Animal Center (Guangdong, China). All animals were acclimatized for one week before the experiments, and fed standard pellets and water ad libitum. The animal room was maintained under a controlled temperature (23 ± 2 °C) with constant light/black cycle (12 h) and humidity (50 ± 10%). All animal experimental protocols were approved by the ethical committee at Guangdong Pharmaceutical University and conducted according to the Laboratory Animal Management Regulations in China and adhered to the Guide for the Care and Use of Laboratory Animals published by the National Institutes of Health (NIH Publication NO. 85-23, revised 2011).

Statistical analyses were performed using GraphPad InStat version 5.00 (San Diego, CA, USA). General effects were analyzed by using a one-way ANOVA with Tukey's multiple-comparison post hoc test.

4.5. Anti-platelet aggregation

Blood were collected from rabbit carotid artery into heparin-containing tubes. After centrifugation at 500 rpm for 10 min to obtain platelet-rich plasma (PRP), the remaining blood was further centrifuged at 3000 rpm for another 10 min to obtain platelet-poor plasma (PPP). PRP was pre-incubated in duplicate for 5 min at 37 °C with vehicle, the tested compounds, or positive control (Ticlopidine) at the concentration of 0.1 mM. Carboxy-PTIO (20 μM) was added and incubated with the drug-platelet suspension in the indicated group. The platelet aggregation in individual PPR samples was induced by ADP (10 μM), followed by recording of light transmission at maximal aggregation within 5 min. The inhibition rate was calculated as following: inhibition rate (%) = (A − B)/A × 100%, A = the platelet aggregation of vehicle group, B = the platelet aggregation of compound group.

4.6. NO release assay

NO release of compound **3** was determined by Griess assay. Briefly, compound **3** (0.03, 0.1, 0.2, and 0.3 mM) in phosphate buffer solution containing 2% dimethyl sulfoxide and 5.0 mM L-cysteine at pH 7.4 was incubated at 37 °C for 15 to 300 min and were sampled every 15 min for 120 min and then every 30 min for the remaining time. The collected samples (2 mL) were mixed with 0.5 mL of Griess reagent and incubated at 37 °C for 10 min, followed by measuring at 550 nm. The different concentrations of nitrite were used as standards to calculate the concentrations of NO.

4.7. Oral glucose tolerance test in mice

Normal male ICR mice (Comparative Medicine Centre of Yangzhou University) after adaptation one week were fasted for 12 h, weighted, bled *via* the tail tip, and randomized into 4 groups (n = 6 per group). Compound **3** (20 mg/kg), TAK-875 (20 mg/kg), or vehicle (0.5% methylcellulose aqueous solution) was orally administered 30 min before oral glucose load (3 g/kg). Blood samples were collected immediately at −30 min (just before drug administration), 0 min (just before glucose challenge), and 15, 30, 60 and 90 min after glucose load. The blood glucose was measured by plasma glucose test strips (SanNuo ChangSha, China).

Acknowledgements

This study was supported by grants from the National Natural Science Foundation of China (Grants 81320108029 and 81773995), the Starting Foundation for Ph.D., Guangdong Pharmaceutical University (Grant 43540073) and Guangdong Province Medical Science and Technology Research Fund (Grant A2018273).

References

[1]. DeFronzo RA. *Diabetes.* 2009;58:773–795.
[2]. Danaei G, Finucane MM, Lu Y, et al. *Lancet.* 2011;378:31–40.
[3]. Phung OJ, Scholle JM, Talwar M, Coleman CI. *JAMA.* 2010;303:1410–1418.
[4]. Avery MA, Mizuno CS, Chittiboyina AG, Kurtz TW, Pershadsingh HA. *Curr Med Chem.* 2008;15:61–74.
[5]. Stein SA, Lamos EM, Davis SN. *Expert Opin Drug Saf.* 2013;12:153–175.
[6]. Lebovitz HE. *Nat Rev Endocrinol.* 2011;7:408–419.
[7]. Inzucchi SE, Bergenstal RM, Buse JB, et al. *Diabetes Care.* 2012;35:1364–1379.
[8]. Matthews DR, Tsapas A. *Diabetes Vasc Dis Res.* 2008;5:216–218.
[9]. Itoh Y, Kawamata Y, Harada M, et al. *Nature.* 2003;422:173–176.
[10]. Briscoe CP, Tadayyon M, Andrews JL, et al. *J Biol Chem.* 2003;278:11303–11311.
[11]. Stoddart LA, Smith NJ, Milligan G. *Pharmacol Rev.* 2008;60:405–417.
[12]. Wellendorph P, Johansen LD, Bräuner-Osborne H. *Mol Pharmacol.* 2009;76:453–465.
[13]. Wang X, Zhao T, Yang B, et al. *Bioorgan Med Chem.* 2015;23:132–140.
[14]. Li Z, Wang X, Xu X, et al. *Bioorgan Med Chem.* 2015;23:7158–7164.
[15]. Negoro N, Sasaki S, Mikami S, et al. *Chem Lett.* 2010;1:290–294.
[16]. Mikami S, Kitamura S, Negoro N, et al. *J Med Chem.* 2012;55:3756–3776.
[17]. Negoro N, Sasaki S, Ito M, et al. *J Med Chem.* 2012;55:1538–1552.
[18]. Houze JB, Zhu L, Sun Y, et al. *Bioorg Med Chem Lett.* 2012;22:1267–1270.
[19]. Brown SP, Dransfield PJ, Vimolratana M, et al. *Chem Lett.* 2012;3:726–730.
[20]. Wang Y, Liu J, Dransfield PJ, et al. *Chem Lett.* 2013;4:551–555.
[21]. McKeown SC, Corbett DF, Goetz AS, et al. *Bioorg Med Chem Lett.* 2007;17:1584–1589.
[22]. Li Z, Qiu QQ, Geng XQ, Yang JY, Huang WL, Qian H. *Expert Opin Inv Drug.* 2016;25:871–890.
[23]. Li Z, Xu X, Huang W, Qian H. *Med Res Rev.* 2018;38:381–425.
[24]. Li Z, Qiu QQ, Xu X, et al. *Eur J Med Chem.* 2016;113:246–257.
[25]. Li Z, Pan MB, Su X, et al. *Bioorgan Med Chem.* 2016;24:1981–1987.
[26]. Li Z, Yang J, Wang X, et al. *Bioorgan Med Chem.* 2016;24:5449–5454.
[27]. Li Z, Yang JY, Gu WJ, et al. *RSC Adv.* 2016;6:46356–46365.
[28]. Li Z, Wang X, Xu X, et al. *Bioorgan Med Chem.* 2015;23:6666–6672.
[29]. Yang J, Li Z, Li H, et al. *Bioorgan Med Chem.* 2017;25:2445–2450.
[30]. Li Z, Liu C, Xu X, et al. *Eur J Med Chem.* 2017;138:458–479.
[31]. Li Z, Liu C, Xu X, et al. *Bioorg Chem.* 2018;76:303–313.
[32]. Li Z, Xu X, Hou J, Wang S, Jiang H, Zhang L. *Bioorg Chem.* 2018;77:429–435.
[33]. Ignarro L. *J Physiol Pharmacol.* 2002;53:503–514.
[34]. Radomski M, Palmer R, Moncada S. *Biochem Biophys Res Commun.* 1987;148:1482–1489.
[35]. Wallace JL. *Mem Inst Oswaldo Cruz.* 2005;100:5–9.
[36]. Srivastava A, Yano J, Hirozane Y, et al. *Nature.* 2014;513:124–127.
[37]. Born GV, Cross MJ. *J. Physiol.* 1963;168:178–195.
[38]. Yin W, Lan L, Huang Z, et al. *Eur J Med Chem.* 2016;115:369–380.